



Published in final edited form as:

Science. 2020 July 24; 369(6502): 450–455. doi:10.1126/science.aaz1333.

## Itaconate is an effector of a Rab GTPase cell-autonomous host defense pathway against *Salmonella*

Meixin Chen<sup>1,4</sup>, Hui Sun<sup>1,4</sup>, Maikel Boot<sup>1</sup>, Lin Shao<sup>1</sup>, Shu-Jung Chang<sup>1</sup>, Weiwei Wang<sup>2</sup>, Tukiet T. Lam<sup>2,3</sup>, Maria Lara-Tejero<sup>1</sup>, E. Hesper Rego<sup>1</sup>, Jorge E. Galán<sup>1,\*</sup>

<sup>1</sup>Department of Microbial Pathogenesis, Yale University School of Medicine, New Haven, CT06536

<sup>2</sup>WM Keck Foundation Biotechnology Resource Laboratory, Yale University School of Medicine, New Haven, CT06536

<sup>3</sup>Department of Molecular Biophysics and Biochemistry, Yale University School of Medicine, New Haven, CT06536

<sup>4</sup>These authors contributed equally

### Abstract

Rab32 coordinates a cell-intrinsic host defense mechanism that restricts the replication of intravacuolar pathogens such as *Salmonella*. Here we show that this mechanism requires itaconate decarboxylase 1 (IRG1), which synthesizes itaconate, a metabolite with antimicrobial activity. We find that Rab32 interacts with IRG1 upon *Salmonella* infection and facilitates the delivery of itaconate to the *Salmonella*-containing vacuole. Mice defective in IRG1 rescued the virulence defect of a *S. Typhimurium* mutant specifically defective in its ability to counter the Rab32 defense mechanism. These studies provide a link between a metabolite produced in the mitochondria after stimulation of innate immune receptors and a cell-autonomous defense mechanism that restricts the replication of an intracellular bacterial pathogen.

### Keywords

innate immunity; bacterial pathogenesis; *Salmonella* pathogenesis; host defense; vesicle transport; Rab32; cell intrinsic immunity; Rab GTPases; mitochondria

---

Many cells are endowed with the capacity to control microbial invaders through cell-intrinsic defense mechanisms that synergize with the immune system to confer whole-body protection (1). Microbial pathogens respond to these host defense strategies by evolving virulence factors that prevent their detection or neutralize the effects of the antimicrobial mechanisms (2). Rab-family GTPases coordinate molecular transport across cellular

---

\* for correspondence: jorge.galan@yale.edu.

**Authors contributions:** M.C. performed most of the experiments, H.S. performed initial experiments, M.B. and L.S. carried out the imaging studies, S.-J.C. assisted M.C. in some experiments, W.W. and T.T.L. performed the itaconate measurements, M.L.-T. performed the LC—MS/MS experiments, E.H.R. supervised the imaging experiments, J.E.G. conceived and directed the project and wrote the manuscript with comments from all the authors.

**Competing interests:** The authors declare no competing interests.

compartments (3). A member of this family, Rab32, orchestrates a cell intrinsic host defense response that restricts the replication of intracellular bacterial pathogens including *Salmonella* Typhi (4–6). *Salmonella* Typhimurium, however, can neutralize this restriction mechanism with two effectors (SopD2 and GtgE) delivered by its type III protein secretion systems (7, 8). The mechanisms by which Rab32 controls bacterial replication are unknown. We hypothesized that Rab32 must control the delivery of an antimicrobial factor(s) to the *Salmonella*-containing vacuole (SCV). However, the nature of any potential factor(s) has remained elusive.

We searched for a cell line in which the Rab32-dependent restriction is robustly manifested by comparing the replication of wild-type *S. Typhimurium* with that of the *gtgE sopD2* mutant, which is unable to neutralize it. We found no difference between the replication of the two strains in mouse embryo fibroblast, HeLa or Henle-407 cells (Fig. 1A–C), even after treatment with interferon (Fig. S1). By contrast, we observed significant differences in murine DC2.4 dendritic cells (Fig. 1D) and, to a lesser extent, in RAW264.7 macrophages (Fig. 1E). Thus, the Rab32 phenotype may be more robustly manifested in cells of hematopoietic origin.

We then searched for Rab32-interacting proteins in DC2.4 cells after infection with the *S. Typhimurium gtgE sopD2* mutant strain at a time of infection that coincides with the recruitment of Rab32 to the SCV (4) (Fig. 1F). A prominent Rab32-interacting protein exclusively detected in infected cells was IRG1 (Fig. 1G, Table S1 and S2). This interaction was confirmed in cells expressing epitope-tagged versions of these proteins (Fig. 1H and Fig. S2) and in DC2.4 cells expressing endogenous *IRG1* (Fig. 1I). The nucleotide state of Rab32 did not appear to affect its interaction with IRG1 (Fig. S3). However, the interaction was enhanced by the bacterial infection (Fig. 1H and 1I and Fig. S2). In addition, *IRG1* expression was detected in *Salmonella*-infected or LPS-treated cells that showed the Rab32-restriction phenotype, but not in cells that did not (Fig. 1J and Fig. S4 and S5). Furthermore, when compared to the wild-type strain, the *S. Typhimurium gtgE sopD2* mutant showed reduced intracellular replication in Henle-407 cells transiently expressing *IRG1* (Fig. S6). IRG1, which is highly expressed in mouse macrophages after stimulation of Toll-like receptors (9), converts cis-aconitate, a tricarboxylic acid cycle intermediate, to itaconic acid (10). By alkylating cysteine residues in the targeted molecules (11, 12), itaconic acid (or itaconate) inhibits methylmalonyl-CoA mutase (13), as well as isocitrate lyase (14) and succinate dehydrogenase (15), essential enzymes in the glyoxylate shunt pathway and the TCA cycle. These pathways are critical for the physiology and pathogenesis of *Salmonella* and *Mycobacterium* spp. (13, 16–20), which are susceptible to the Rab32-mediated defense mechanism (4, 7, 21). Furthermore, itaconic acid inhibits the growth of *Mycobacterium* spp., *S. Typhimurium* (10) and *S. Typhi* (Fig. S7).

To investigate whether itaconic acid is delivered to the (SCV), we developed a biosensor to report the presence of itaconic acid in *Salmonella*. *S. Typhimurium* encodes a putative itaconate-degradation pathway (22), which is absent from *S. Typhi* (Fig. 2A). By analogy to similar systems in other bacteria (23), expression of this pathway is expected to be controlled by a transcriptional regulatory protein (STM3121), which directly senses itaconic acid (Fig. 2A). We constructed a transcriptional reporter in which the expression of the green

fluorescent protein (GFP), or nanoluciferase was placed under the control of a promoter whose expression is directly controlled by STM3121 (Fig. 2A). The reporters responded to the presence of itaconic acid in a dose-dependent manner (Fig. 2B and 2C), maintaining a linear response up to itaconate concentrations of ~5–6 mM (Fig. S8). The reporter's response was specific as addition of other metabolites or environmental stimuli did not result in a measurable transcriptional response (Fig. S9). We then tested whether itaconic acid was delivered to the SCV and whether the reporter strains could sense its presence within this environment. Infection of cells, which do not express *IRG1* (Fig. 1), with *Salmonella* strains encoding the itaconate reporters, did not result in any measurable production of nanoluciferase (Fig. 2D and Fig. S10 and S11) or GFP (Fig. 2E and Fig. S12). By contrast, infection of cells that express *IRG1* resulted in robust expression of the reporters (Fig. 2D, 2E, and Fig. S9, S10, and S11). Based on the dose response of the reporter (Fig. S8), the concentration of itaconate within the SCV is estimated to be ~6 mM, a concentration predicted to inhibit *Salmonella* growth (Fig. S7).

We then examined whether the Rab32 pathway influences the production or the delivery of itaconate to the SCV. We reasoned that if the Rab32 pathway influences the presence of itaconate in the SCV, wild-type *S. Typhimurium* should impair this process by the action of SopD2 and GtgE (4, 7). Consistent with this hypothesis, expression of the itaconate biosensor was detected at significantly reduced levels in DC2.4 or RAW264.7 cells infected with wild type bacteria in comparison to the *gtgE sopD2* mutant strain (Fig. 3A and Fig. S13), despite equivalent levels of *IRG1* expression in the infected cells (Fig. S14). We then compared the expression of the itaconate reporter in bone marrow derived macrophages (BMDMs) obtained from C57BL/6, *IRG1*<sup>-/-</sup>, BLOC3 deficient (*Hsp4*<sup>-/-</sup>) [the exchange factor for Rab32 (24)], or *Rab32*<sup>-/-</sup> mice, after infection with different *Salmonella* reporter strains. We found robust expression of the itaconate biosensor after infection of BMDMs obtained from C57BL/6 but not in BMDMs obtained from *IRG1*-defective mice (Fig. 3B–D). Importantly, expression of the reporter was detected at significantly reduced levels in BMDMs obtained from *Hsp4*<sup>-/-</sup> or *Rab32*<sup>-/-</sup> mice. Expression of the reporter in *Rab32*<sup>-/-</sup> BMDMs was higher than in *Hsp4*<sup>-/-</sup> BMDMs, suggesting that in the absence of Rab32, the related Rab38 GTPase may partially compensate for its function (Fig. 3B–D). The levels of itaconate in BMDMs obtained from C57BL/6, *IRG1*<sup>-/-</sup>, *Hsp4*<sup>-/-</sup>, or *Rab32*<sup>-/-</sup> mice after stimulation with LPS were indistinguishable from one another (Fig. 3E and Table S3), indicating that the delivery of itaconate to the SCV, not its synthesis, is dependent on the Rab32—BLOC3 pathway.

A proportion of the intracellular *Salmonella* breaks from the SCV to the cell cytosol where it can replicate at a faster rate (25). To investigate whether delivery of itaconate requires the integrity of the SCV, we examined the expression of the itaconate reporter in intravacuolar and cytoplasmic bacteria. Expression of *S. Typhi*'s typhoid toxin requires the environment of the SCV thus serving as a marker to distinguish intravacuolar vs intracytosolic bacteria (26). We found that all bacteria expressing the itaconate reporter were located within the SCV while no bacteria found within the cytosol showed expression of the reporter (Fig. 3F and Fig. S15).

The transport of mitochondria-originated products to other vesicular compartment is well documented (27, 28). As Rab32 is present in the mitochondria (29) and the SCV (4), this GTPase may aid the formation and/or delivery of itaconate and/or IRG1-transport carriers, or it may facilitate the tethering of the mitochondria with the SCV. We used live-cell time-lapse fluorescence microscopy to examine cells stably expressing GFP-tagged IRG1 that had been infected with *Salmonella* expressing an mCherry itaconate reporter. We found that in uninfected cells, IRG1 was uniformly distributed throughout the entire mitochondrial network (Fig. S16 and Table S4). After *Salmonella* infection, we observed many instances in which the IRG1-containing mitochondrial network repositioned to surround and make intimate contact with the SCV, a process that coincided with the activation of the itaconate biosensor in the intracellular bacteria (Fig. 3G, and videos S1–S3). Examination of the infected cells by two-color 3D super-resolution structured-illumination microscopy (3D-SIM) (30) revealed intimate contact between the IRG1-containing mitochondrial network and the SCV (Fig. 3H and videos S4–S7). These observations suggest a mechanism by which the close association between the IRG1-containing mitochondria and the SCV may facilitate their tethering and subsequent itaconate transport.

We compared the ability of wild-type *S. Typhimurium* or the *sopD2 gtgE* mutant to replicate within BMDMs obtained from C57BL/6, *IRG1*<sup>-/-</sup>, or *Hsp4*<sup>-/-</sup> mice. As previously shown (7), the *S. Typhimurium sopD2 gtgE* mutant exhibited reduced ability to replicate within C57BL/6 BMDMs, and this phenotype was rescued in BMDMs obtained from *Hsp4*<sup>-/-</sup> animals (Fig. 4A). Importantly, the replication-deficient phenotype was also rescued in BMDMs obtained from *IRG1*<sup>-/-</sup> mice, which allowed the replication of the *S. Typhimurium sopD2 gtgE* mutant to levels almost equivalent to those of wild type bacteria (Fig. 4A). The human-adapted pathogen *S. Typhi* is unable to replicate in mouse macrophages because the Rab32—BLOC3 pathway restricts its replication (4). As we have previously shown (4), *S. Typhi* was able to replicate in BMDMs from *Hsp4*<sup>-/-</sup> mice to levels almost equivalent to those of wild-type *S. Typhimurium* (Fig. 4B). Importantly, *S. Typhi* was able to replicate in BMDMs from *IRG1*<sup>-/-</sup> mice although not to the same extent as to the levels observed in BMDMs from *Hsp4*<sup>-/-</sup> mice (Fig. 4B). This suggests that, in addition to itaconate, the Rab32—BLOC3 pathway may deliver additional antimicrobial factors. The *S. Typhimurium sopD2 gtgE* mutant exhibits significantly reduced mouse virulence when compared to the wild-type strain and the virulence defect can be reversed in BLOC3-defective mice (7). We therefore reasoned that if itaconate is an effector of this pathway, the virulence attenuation of the *S. Typhimurium sopD2 gtgE* mutant strain should be reversed in *IRG1*<sup>-/-</sup> mice. Consistent with this hypothesis, the virulence defect of the *S. Typhimurium sopD2 gtgE* mutant was significantly reversed in *IRG1*<sup>-/-</sup> mice (Fig. 4C). We also examined whether the deployment of the SopD2/GtgE effectors was able to blunt the delivery of itaconate to the SCV during infection. We found that twenty-four hours after infection, the itaconate reporter activity was almost undetectable in the spleens of animals infected with wild type *S. Typhimurium*. By contrast, significantly higher activity was detected in the spleens of animals infected with the *sopD2 gtgE* mutant strain (Fig. 4D).

We have shown here that itaconate is an effector of the Rab32-dependent pathogen restriction pathway that limits the replication of *Salmonella* (Fig. 4E). In phagocytic cells, itaconate can also be delivered to vacuoles containing other bacteria (e.g. *Escherichia coli*)

or avirulent *S. Typhi* lacking its two type III secretion systems (Fig. S17). We therefore hypothesized that this is a general mechanism of defense that may participate in the restriction of other vacuolar pathogenic bacteria. How itaconate inhibits bacterial growth is likely to be multi-factorial, exerting its function by altering bacterial metabolism through its ability to inhibit key metabolic enzymes. Although itaconate has also been reported to have modulatory activities over multicellular responses including inflammation (31), it is unlikely that those activities are central to the Rab32—BLOC3-mediated pathogen restriction mechanism, which involves the direct delivery of this metabolite to the bacterial-containing vacuole. These studies emphasize the critical role played by mitochondria in the control of microbial infections and the Rab32 pathway as a major link between this organelle and the compartments housing bacterial pathogens.

## Supplementary Material

Refer to Web version on PubMed Central for supplementary material.

## Acknowledgment

We thank Dr. M. Diamond and Dr. M. Artyomov for facilitating the *Irg1<sup>-/-</sup>* mouse. Funding: The Proteomics Resource of the WM Keck Foundation Biotechnology Resource Laboratory was partially supported by CTSA Grant Number UL1TR001863 from the National Center for Advancing Translational Sciences (NCATS) of the National Institutes of Health (NIH). This work was supported by NIH Grants R01AI114618 and R01AI055472 to J.G.

## Data and materials availability:

all data are available in the main text, supplementary materials, and auxiliary files.

## References and Notes

1. Randow F, MacMicking J, James L, Cellular self-defense: how cell-autonomous immunity protects against pathogens. *Science* 340, 701–706. (2013). [PubMed: 23661752]
2. Reddick L, Alto N, Bacteria fighting back: how pathogens target and subvert the host innate immune system. *Mol Cell*. 54, 321–328 (2014). [PubMed: 24766896]
3. Stenmark H, Rab GTPases as coordinators of vesicle traffic. *Nat Rev Mol Cell Biol*. 10, 513–525 (2009). [PubMed: 19603039]
4. Spanò S, Galán J, A Rab32-dependent pathway contributes to *Salmonella typhi* host restriction. *Science* 338, 960–963 (2012). [PubMed: 23162001]
5. Tang B, Rab32/38 and the xenophagic restriction of intracellular bacteria replication. *Microbes Infect*. 18, 595–603 (2016). [PubMed: 27256464]
6. Li Y et al., Analysis of the Rab GTPase Interactome in Dendritic Cells Reveals Antimicrobial Functions of the Rab32 Complex in Bacterial Containment. *Immunity* 44, 422–437 (2016). [PubMed: 26885862]
7. Spanò S, Gao X, Hannemann S, Lara-Tejero M, Galán J, A Bacterial Pathogen Targets a Host Rab-Family GTPase Defense Pathway with a GAP. *Cell Host Microbe* 19, 216–226 (2016). [PubMed: 26867180]
8. Spano S, Liu X, Galan JE, Proteolytic targeting of Rab29 by an effector protein distinguishes the intracellular compartments of human-adapted and broad-host *Salmonella*. *Proc Natl Acad Sci U S A* 108, 18418–18423 (2011). [PubMed: 22042847]
9. Lee C, Jenkins N, Gilbert D, Copeland N, O'Brien W, Cloning and analysis of gene regulation of a novel LPS-inducible cDNA. *Immunogenetics* 41, 263–270 (1995). [PubMed: 7721348]

10. Michelucci A et al., Immune-responsive gene 1 protein links metabolism to immunity by catalyzing itaconic acid production. *Proc Natl Acad Sci U S A.* 110, 7820–7825 (2013). [PubMed: 23610393]
11. Mills E et al., Itaconate is an anti-inflammatory metabolite that activates Nrf2 via alkylation of KEAP1. *Nature* 556, 113–117 (2018). [PubMed: 29590092]
12. Bambouskova M et al., Electrophilic properties of itaconate and derivatives regulate the I $\kappa$ B $\zeta$ -ATF3 inflammatory axis. *Nature* 556, 501–504 (2018). [PubMed: 29670287]
13. Ruetz M et al., Itaconyl-CoA forms a stable biradical in methylmalonyl-CoA mutase and derails its activity and repair. *Science* 366, 589–593 (2019). [PubMed: 31672889]
14. McFadden B, Purohit S, Itaconate, an isocitrate lyase-directed inhibitor in *Pseudomonas indigofera*. *J Bacteriol.* 131, 136–144 (1977). [PubMed: 17593]
15. Cordes T et al., Immunoresponsive Gene 1 and Itaconate Inhibit Succinate Dehydrogenase to Modulate Intracellular Succinate Levels. *J Biol Chem.* 291, 14274–14284 (2016). [PubMed: 27189937]
16. Wilson R, Maloy S, Isolation and characterization of *Salmonella typhimurium* glyoxylate shunt mutants. *J Bacteriol.* 169, 3029–3034 (1987). [PubMed: 3298210]
17. Fang F, Libby S, Castor M, Fung A, Isocitrate lyase (AceA) is required for *Salmonella* persistence but not for acute lethal infection in mice. *Infect Immun.* 73, 2547–2549 (2005). [PubMed: 15784602]
18. McKinney J et al., Persistence of *Mycobacterium tuberculosis* in macrophages and mice requires the glyoxylate shunt enzyme isocitrate lyase. *Nature* 406, 735–738 (2000). [PubMed: 10963599]
19. Mercado-Lubo R, Gauger E, Leatham M, Conway T, Cohen P, A *Salmonella enterica* serovar typhimurium succinate dehydrogenase/fumarate reductase double mutant is avirulent and immunogenic in BALB/c mice. *Infect. Immun.* 76, 1128–1134 (2008). [PubMed: 18086808]
20. Hartman T et al., Succinate dehydrogenase is the regulator of respiration in *Mycobacterium tuberculosis*. *PLoS Pathog.* 10, e1004510 (2014). [PubMed: 25412183]
21. Zhang F et al., Identification of two new loci at IL23R and RAB32 that influence susceptibility to leprosy. *Nat Genet* 43, 1247–1251 (2011). [PubMed: 22019778]
22. Sasikaran J, Ziemski M, Zadora P, Fleig A, Berg I, Bacterial itaconate degradation promotes pathogenicity. *Nat. Chem. Biol.* 10, 371–377 (2014). [PubMed: 24657929]
23. Hanko E, Minton N, Malys N, A Transcription Factor-Based Biosensor for Detection of Itaconic Acid. *ACS Synth Biol.* 7, 1436–1446 (2018). [PubMed: 29638114]
24. Gerondopoulos A, Langemeyer L, Liang J, Linford A, Barr F, BLOC-3 mutated in Hermansky-Pudlak syndrome is a Rab32/38 guanine nucleotide exchange factor. *Curr Biol.* 22, 2135–2139 (2012). [PubMed: 23084991]
25. Knodler L, *Salmonella enterica*: living a double life in epithelial cells. *Curr Opin Microbiol.* 23, 23–31 (2015). [PubMed: 25461569]
26. Fowler C, Galán J, Decoding a *Salmonella* Typhi Regulatory Network that Controls Typhoid Toxin Expression within Human Cells. *Cell Host Microbe* 23, 65–76 (2018). [PubMed: 29324231]
27. Soto-Herederó G, Baixauli F, Mittelbrunn M, Interorganellar Communication between Mitochondria and the Endolysosomal System. *Front. Cell Dev. Biol.* 5, 95 (2017). [PubMed: 29164114]
28. Abuaita B, Schultz T, O’Riordan M, Mitochondria-Derived Vesicles Deliver Antimicrobial Reactive Oxygen Species to Control Phagosome-Localized *Staphylococcus aureus*. *Cell Host Microbe.* 24, 625–636 (2018). [PubMed: 30449314]
29. Alto N, Soderling J, Scott J, Rab32 is an A-kinase anchoring protein and participates in mitochondrial dynamics. *J Cell Biol.* 158, 659–668 (2002). [PubMed: 12186851]
30. Gustafsson M et al., Three-dimensional resolution doubling in wide-field fluorescence microscopy by structured illumination. *Biophys J.* 94, 4957–4970 (2008). [PubMed: 18326650]
31. Yu X, Zhang D, Zheng X, Tang C, Itaconate: an emerging determinant of inflammation in activated macrophages. *Immunol Cell Biol.* 97, 134–141 (2019). [PubMed: 30428148]
32. Gibson D et al., Enzymatic assembly of DNA molecules up to several hundred kilobases. *Nat Methods.* 6, 343–345 (2009). [PubMed: 19363495]

33. Fowler C, Galán J, Decoding a Salmonella Typhi Regulatory Network that Controls Typhoid Toxin Expression within Human Cells. *Cell Host Microbe* 23, 65–76 (2018 ). [PubMed: 29324231]
34. Fitzsimmons L et al., Zinc-dependent substrate-level phosphorylation powers Salmonella growth under nitrosative stress of the innate host response. *PLoS Pathog.* 14, e1007388 (2018 ). [PubMed: 30365536]
35. Fiolka R, Shao L, Rego E, Davidson M, Gustafsson M, Time-lapse two-color 3D imaging of live cells with doubled resolution using structured illumination. *Proc Natl Acad Sci U S A.* 109, 5311–5315 (2012 ). [PubMed: 22431626]
36. Schindelin J et al., Fiji: an open-source platform for biological-image analysis. *Nat Methods.* 9, 676–682 (2012). [PubMed: 22743772]
37. Lampropoulou V et al., Itaconate Links Inhibition of Succinate Dehydrogenase with Macrophage Metabolic Remodeling and Regulation of Inflammation. *Cell Metab.* 24, 158–166 (2016 ). [PubMed: 27374498]

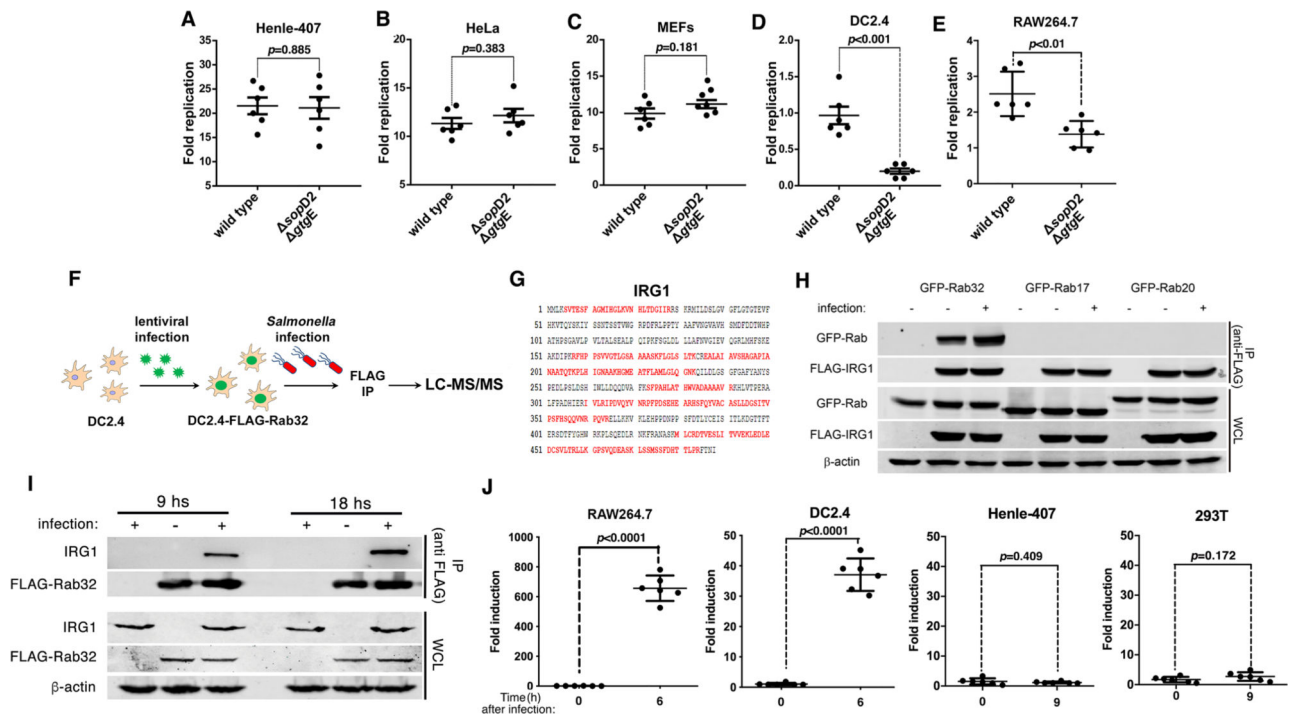


**Fig. 1. IRG1 interacts with Rab32 during *Salmonella* infection.**

(A-E) The Rab32-associated pathogen restriction mechanism is manifested in myelocytic but not in epithelial cell lines. The ability of the *S. Typhimurium* *sopD2 gtgE* mutant strain to replicate within epithelial (Henle-407 and HeLa) or myelocytic (DC2.4 and RAW264.7) cell lines was evaluated by determining the CFU at different times after infection (MOI = 5). Fold replication represents the difference between the CFU at 1 and 9 hours post infection. Each circle represents the fold replication in each individual determination; the mean  $\pm$  SEM of all the measurements and the  $p$  values of the indicated comparisons (two-sided Student's  $t$ -test) are shown. (F-I) Rab32 interacts with IRG1 after *Salmonella* infection. DC2.4 cells expressing endogenous levels of FLAG-tagged Rab32 were infected with *S. Typhimurium* *sopD2 gtgE* (MOI = 30) and Rab32-interacting proteins were identified by affinity purification and LC-MS/MS analysis (F). The IRG1 peptides identified by the analyses are shown in red (G). (H and I) HEK293T cells transiently co-transfected with a plasmid expressing GFP-tagged Rab32, Rab17, or Rab20, along with a plasmid encoding FLAG-tagged IRG1 (H), or DC2.4 cells stably expressing FLAG-tagged Rab32 (I) were infected with *S. Typhimurium* *gtgE sopD2* for 4 hours (MOI = 5). Cell lysates were then analyzed by immunoprecipitation with anti-FLAG and immunoblotting with anti-GFP, anti-FLAG, anti-IRG1, or anti- $\beta$ -actin (as loading control) antibodies. IP: immunoprecipitates; WCL: whole-cell lysates. (J) Expression of *IRG1* after *Salmonella* infection. The indicated cell lines were infected with *S. Typhimurium* *sopD2 gtgE* mutant strain (MOI = 5) and *IRG1* mRNA levels were measured by qPCR 6 or 9 hours after infection. Each circle represents a single determination of the relative levels of *IRG1* normalized to the levels of GAPDH; the mean  $\pm$  SEM of all the measurements and  $p$  values of the indicated comparisons (two-sided Student's  $t$  test) are shown.



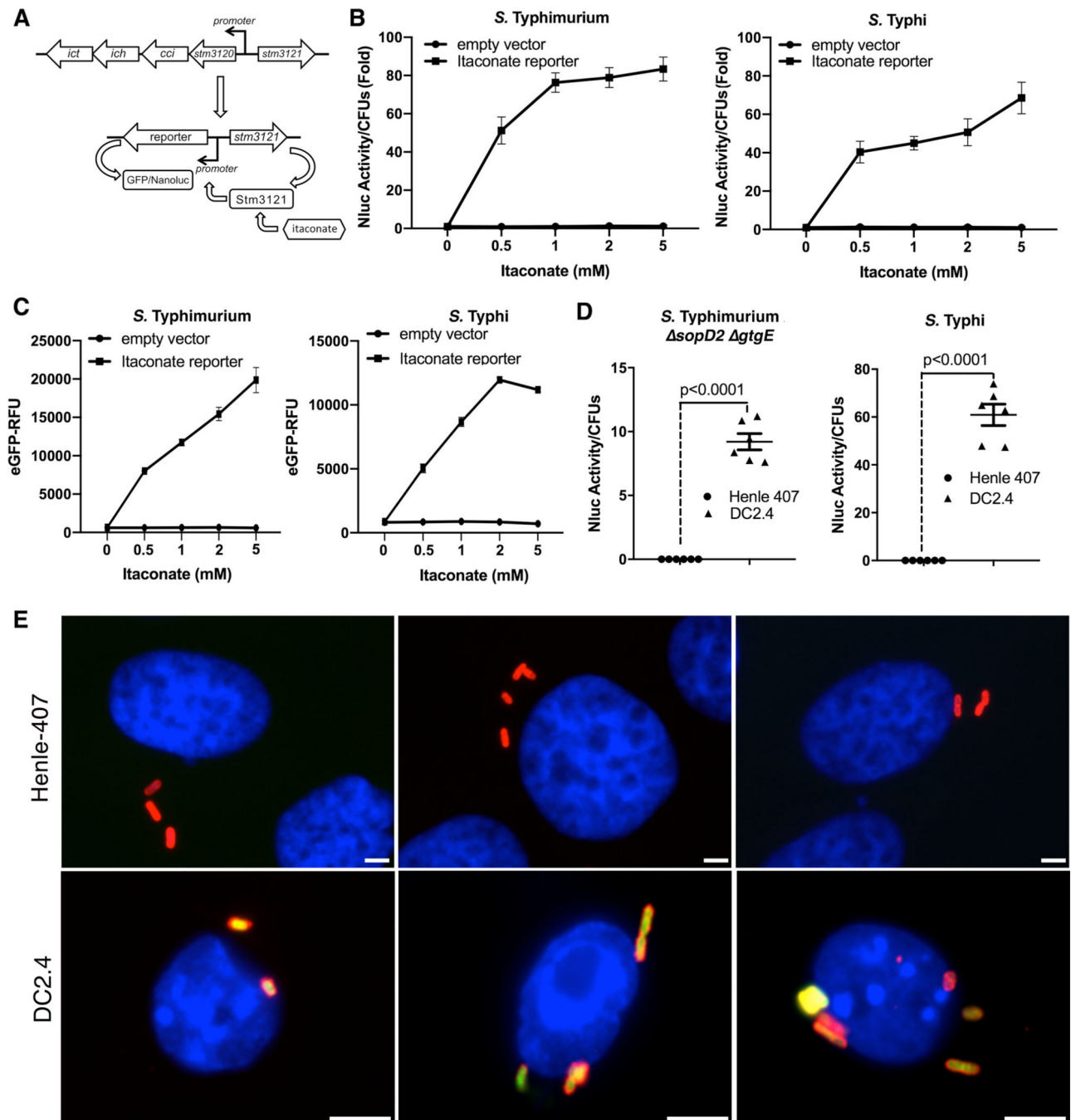


**Fig. 2. Itaconate is delivered to the *Salmonella*-containing vacuole.**

(A-C). Development of a biosensor to detect itaconate. (A) Chromosomal organization of the itaconate-degradation gene cluster in *S. Typhimurium* and diagram of the itaconate biosensor. (B and C) Effect of addition of itaconate on the biosensor transcriptional response. *S. Typhimurium* and *S. Typhi* strains carrying either the nanoluciferase or eGFP itaconate reporters were grown to an OD<sub>600</sub> of 0.9 in the presence of different concentrations of itaconic acid (as indicated) and the levels of nanoluciferase or eGFP were determined. Values are the mean  $\pm$  SD of three independent measurements. This experiment was

repeated at least three times with equivalent results. **(D and E)** Detection of itaconate by intracellular *Salmonella*. DC2.4 or Henle-407 cells were infected with a *S. Typhimurium* *sopD2 gtgE* mutant (MOI=5) or *S. Typhi* (MOI=10) carrying a plasmid encoding a nanoluciferase-based itaconate biosensor. Eighteen hours after infection, the levels of nanoluciferase were measured in lysates of the infected cells **(D)**. Each circle or triangle represents a single luciferase measurement; the mean  $\pm$  SD and *p* values of the indicated comparisons (two-sided Student's *t* test) are shown. This experiment was repeated at least three times with equivalent results. Alternatively, DC2.4 or Henle-407 cells were infected (MOI = 10) with *S. Typhi* carrying a plasmid encoding the eGFP-based itaconate biosensor (green). Eighteen hours after infection, cells were fixed, stained with DAPI (blue) to visualize nuclei, and stained with an anti-*Salmonella* LPS antibody along with Alexa 594-conjugated anti-rabbit antibody (red), and imaged under a fluorescence microscope **(E)**. Scale bars: 5  $\mu$ m.

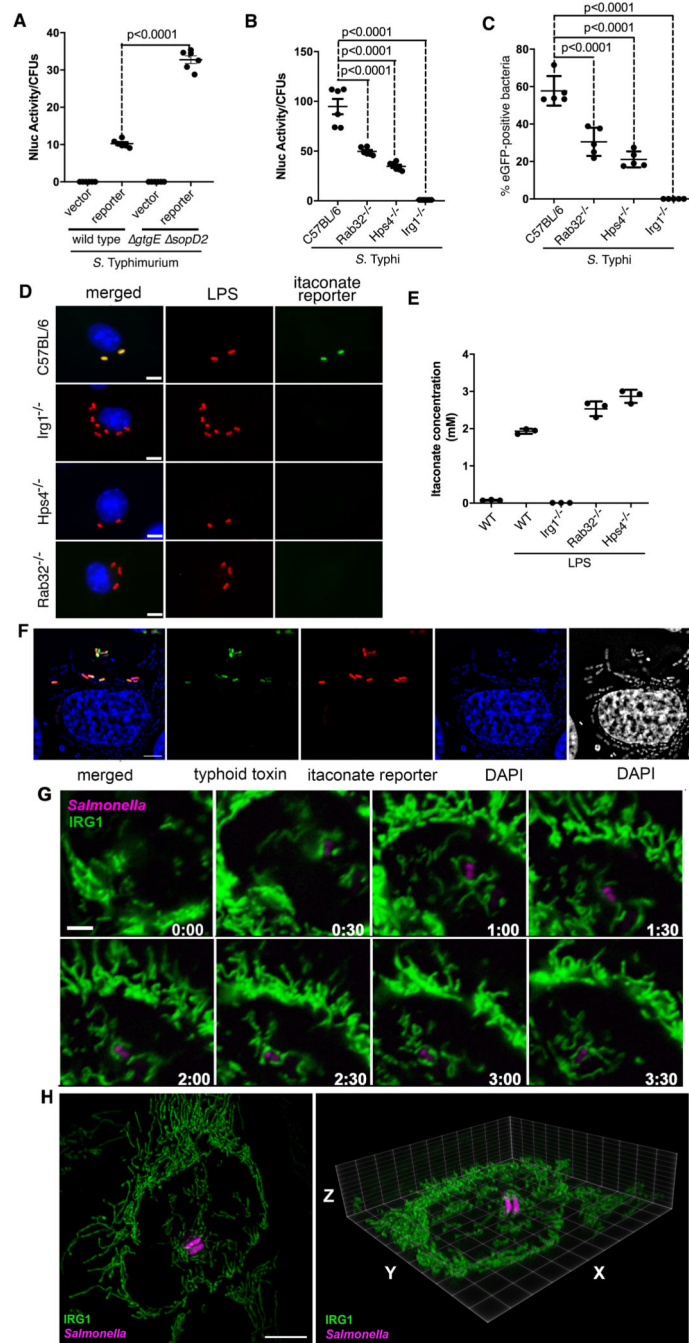


**Fig. 3. Rab32/BLOC3-dependent delivery of itaconate to the *Salmonella*-containing vacuole.** (A) Cultured DC2.4 cells were infected with wild-type or *gtgE sopD2* *S. Typhimurium* strains (MOI = 5) encoding the luciferase-based itaconate biosensor and the levels of luciferase in cell lysates were measured 9 hours after infection. Each circle represents a single luciferase measurement; the mean  $\pm$  SD and the *p*-values of the indicated comparisons (two-sided Student's *t*-test) are shown. (B-D) Bone-marrow-derived macrophages (BMDMs) obtained from C57BL/6, Rab32<sup>-/-</sup>, Hsp4<sup>-/-</sup>, or IRG1<sup>-/-</sup> mice were infected with *S. Typhi* (MOI = 10) encoding the luciferase- or eGFP-based itaconate biosensors. Nine hours after

infection, the levels of luciferase in cell lysates (**B**) or the number of cells expressing eGFP (**C**) were determined. Each circle in (**B**) represents a single luciferase measurement. Values in (**C**) represent the percentage of bacterial cells exhibiting fluorescence. A minimum of 200 cells in each condition was evaluated. The mean  $\pm$  SD and *p*-values of the indicated comparisons (one-way Anova) are shown. Representative fields of BMDMs obtained from the indicated mouse lines infected with *S. Typhi* encoding the eGFP itaconate reporter (green) are shown. Cells were fixed, stained with DAPI (blue) to visualize nuclei and stained with an anti-*Salmonella* LPS antibody along with Alexa 594-conjugated anti-rabbit antibody (red) (**D**) (scale bar = 5  $\mu$ m). (**E**) Itaconate levels in BMDMs obtained from the indicated mice before and after LPS treatment to induce the expression of IRG1. Values represent the mean  $\pm$  SD of three independent measurements. (**F**) Expression of the itaconate reporter (red) by intravacuolar but not by cytosolic *S. Typhi*. HeLa cells transfected with a plasmid encoding FLAG-tagged IRG1 were infected by a *S. Typhi* strain encoding a mCherry itaconate reporter (red) and a *pltB::GFP* transcriptional reporter (green). PltB, a component of *S. Typhi*'s typhoid toxin, is exclusively produced by bacteria located within the SCV and therefore serves as a surrogate to report for intravacuolar (GFP positive) vs intra cytosolic (GFP negative) bacteria. Six hours after infection, cells were stained with DAPI (to visualize all bacteria) and examined under a fluorescence microscope (scale bars: 5  $\mu$ m). (**G**) Live-cell fluorescence time-lapse microscopy of cultured HeLa cells stably expressing IRG1-GFP (green) infected with *S. Typhimurium gtgE sopD2* mutant strain encoding an mCherry itaconate biosensor (magenta). Imaging was initiated 45 minutes after infection. The times (hours:min) after initiation of imaging are indicated in each frame (the entire sequence is shown in video S1; this experiment was conducted at least three independent times, imaging several independent positions in each experiment, with equivalent findings; see videos S2 and S3 for additional examples). (**H**) Snapshot of a 3-D rendering of 3D-SIM acquisitions of HeLa cells stably expressing IRG1-GFP (green) infected with *S. Typhimurium gtgE sopD2* mutant strain encoding an mCherry itaconate biosensor (magenta) (videos of this and additional reconstructions can be found in videos S4–S7).

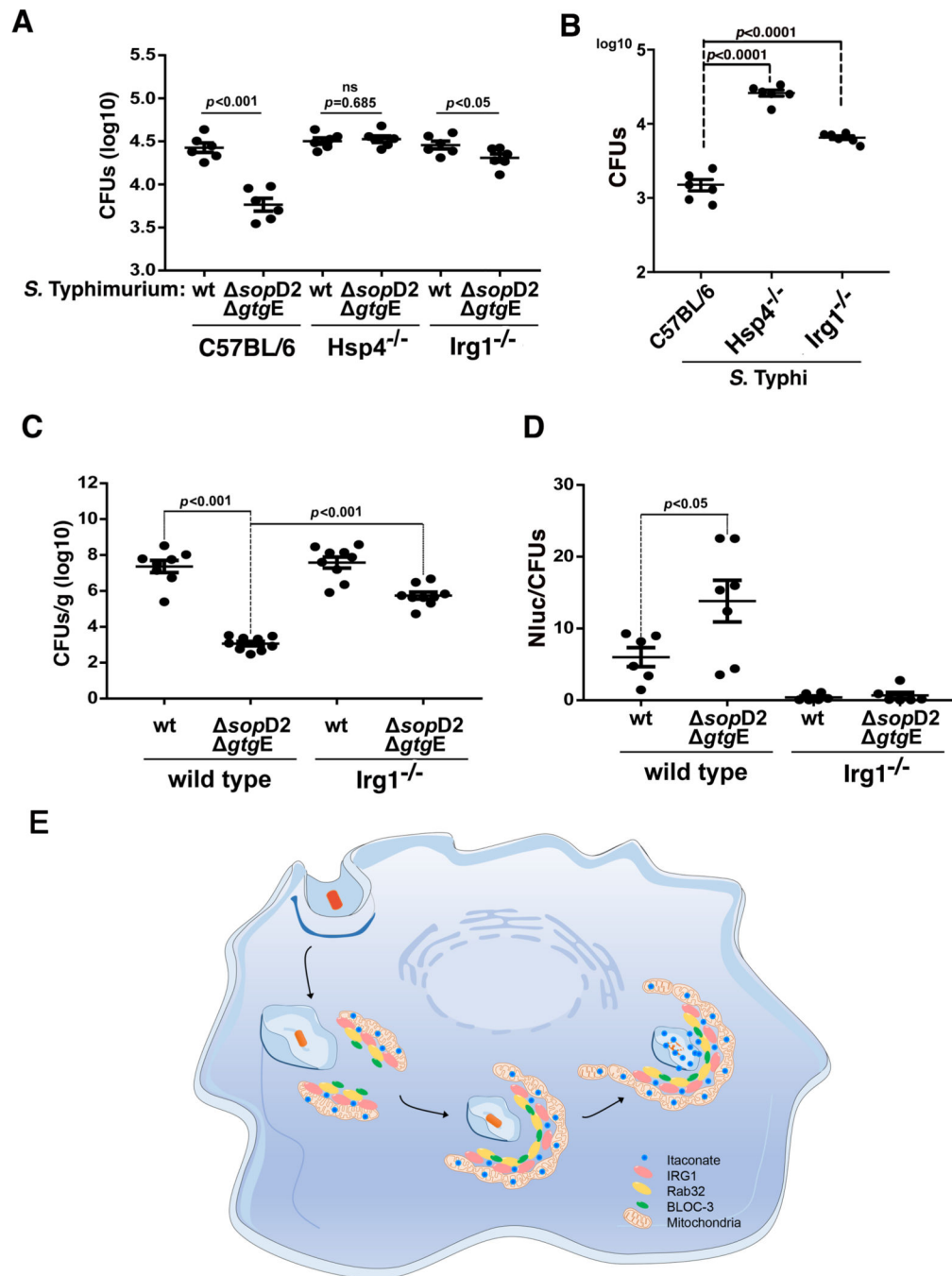


**Fig. 4. Susceptibility of IRG1-deficient mice to *Salmonella* infection.**

(A and B) Bone-marrow-derived macrophages (BMDMs) obtained from C57BL/6 (WT), *Hsp4*<sup>-/-</sup>, or *IRG1*<sup>-/-</sup> mice were infected with wild-type *S. Typhimurium* (MOI=5), its *gtgE sopD2* mutant derivative (MOI=5) (A), or wild-type *S. Typhi* (MOI=10) (B), and the number of CFU was determined 9 hours after infection. Each circle represents the CFU in independent measurements; the mean  $\pm$  SEM of all the measurements and *p*-values of the indicated comparisons (two-sided Student's *t* test) are shown. (C and D) C57BL/6 (wild-type) or *IRG1*<sup>-/-</sup> mice were intraperitoneally infected with wild-type or *gtgE sopD2 S.*

Typhimurium (as indicated) ( $10^2$  CFU). Five days after infection, bacterial loads in the spleen of the infected animals were determined (**C**). Alternatively, mice were intraperitoneally infected with the same strains ( $10^4$  CFU) and the levels of luciferase activity in spleen lysates was quantified 24 hours after infection (**D**). Each circle in (**C**) represents the bacterial loads of the spleen of an individual animal, and in (**D**) represents the luciferase levels in the spleen of an individual animal normalized to the CFU. The mean  $\pm$  SEM of all the determination and  $p$ -values of the indicated comparisons (two-sided Student's  $t$ -test) are shown. (**E**) Model for the mechanism of Rab32—BLOC3-mediated itaconate delivery to the Salmonella-containing vacuole. Upon infection, the mitochondrial network repositions to surround the incoming bacteria, and the resulting close interaction between the mitochondria and the *Salmonella*-containing vacuole results in the Rab32—BLOC3 dependent delivery of itaconate, which is synthesized in the mitochondria by IRG1.